

1997

Alloy Oxidation and Porcelain Fused to Alloy Interaction in Noble Alloy Systems

M. S. Bapna
University of Illinois

H. J. Mueller
American Dental Association

Follow this and additional works at: <https://digitalcommons.usu.edu/cellsandmaterials>



Part of the [Biomedical Engineering and Bioengineering Commons](#)

Recommended Citation

Bapna, M. S. and Mueller, H. J. (1997) "Alloy Oxidation and Porcelain Fused to Alloy Interaction in Noble Alloy Systems," *Cells and Materials*: Vol. 7 : No. 1 , Article 1.

Available at: <https://digitalcommons.usu.edu/cellsandmaterials/vol7/iss1/1>

This Article is brought to you for free and open access by the Western Dairy Center at DigitalCommons@USU. It has been accepted for inclusion in Cells and Materials by an authorized administrator of DigitalCommons@USU. For more information, please contact digitalcommons@usu.edu.



ALLOY OXIDATION AND PORCELAIN FUSED TO ALLOY INTERACTION IN NOBLE ALLOY SYSTEMS

M.S. Bapna^{1,*} and H.J. Mueller^{2,3}

¹Division of Biomaterials, University of Illinois College of Dentistry, Chicago, Illinois

²Department of Dental Biomaterials, American Dental Association, Chicago, Illinois

³Current address: Paffenbarger Res. Ctr., Natl. Inst. Standards and Technology, Gaithersburg, MD

(Received for publication January 24, 1997 and in revised form August 13, 1997)

Abstract

The oxidation and porcelain fusion characteristics of noble alloys containing a variety of minor oxidizable elements, including Cu, Sn, In, Ga, Mn, and Fe were investigated. Four porcelain alloys systems: a Pd-base alloy (Naturelle), two Pd-Ag-based alloys (Jelstar and Acclaim), and a high Au-alloy (SMG-3) were examined by scanning electron microscopy and energy dispersive spectroscopy after being heat treated and after being fused with porcelain. Internal oxidation of minor alloying elements occurred within several micrometers from the surface in all four alloys. Surface nodules as detected by other investigators for a Pd-Ag alloy were also detected in this study. Evidence for occurrence of such nodules in the high Au-content alloy were also noted. Naturelle, a high Ga and Cu containing alloy, was also characterized by the presence of a $Ga_2O_3 \cdot CuO$ layer beneath Pd-Cu nodules and at grain boundaries. A surface oxide layer, as thin as 100 nm, of $Fe_2O_3 \cdot SnO_2$ was observed in the high Au-alloy. The morphologies for alloy/porcelain interfaces were similar. The presence of minor alloying elements was observed within a distance of several micrometers in the porcelain from the alloy/porcelain interface. These results suggest a predominantly mechanical bond with Pd-Ag base alloys (Jelstar and Acclaim) while a significant contribution by a chemical bond in Pd-base (Naturelle) and high Au-alloy (SMG-3).

Key Words: Palladium base alloys, alloy oxidation, fusion, porcelain-alloy interaction, scanning electron microscopy, energy dispersive spectroscopy, interface, diffusion, bonding.

*Address for correspondence:

M. S. Bapna

Division of Biomaterials, Dept. of Restorative Dentistry
University of Illinois, College of Dentistry

801 S. Paulina Street, Chicago, IL 60612-7210

Telephone no.: 312-996-5697 / FAX no.: 312-996-3535

E-mail: bapnam@uic.edu

Introduction

In recent years, a variety of new or modified dental alloy systems based upon palladium, nickel-cobalt, titanium and low gold content have become commercially available for ceramic veneering. Alloy development occurred either to find an alternative to the more expensive gold alloys and/or an esthetically favorable alloy system with improved alloy/porcelain interface bond. Several theories have been put forward to explain the bonding mechanisms between porcelain and the alloy substrate (Fairhurst, 1977; Pask, 1977; Mackert *et al.*, 1984, 1988; Anusavice, 1985; Baran, 1985; Fairhurst *et al.*, 1985; Tomsia and Pask, 1986; Pask and Tomsia, 1988; O'Connor *et al.*, 1996). Earlier investigations have shown that the alloy surface oxidation during the initial heat treatment plays an important role in the bonding of porcelain to the alloy (King *et al.*, 1959; Borom and Pask, 1966; Lautenschlager *et al.*, 1969; von Radnoth *et al.*, 1969; Laub *et al.*, 1978; Ohno *et al.*, 1981). The small amount of base metals such as Sn, In, Fe, Mn, Ga, etc. in the alloy oxidizes selectively during the heat treatment and contributes by one or a combination of the several mechanisms to the alloy-porcelain interface bond (Nally, 1968; Lautenschlager *et al.*, 1969; Anusavice *et al.*, 1977; Miyagawa, 1978; Stewart *et al.*, 1978; Ohno *et al.*, 1982, 1983; Sarkar *et al.*, 1985; Vrijhoef and van Der Zel, 1988; Hautaniemi *et al.*, 1990). The enhanced wettability of porcelain on the oxidized alloy surface, the mechanical lock formation at an alloy-porcelain interface, and the chemical interaction between the alloy surface oxides and the oxides in porcelain are processes considered for improved bond strength (Zacky *et al.*, 1953; King *et al.*, 1959; Pask and Fulrath, 1962; Pask, 1977; Mackert *et al.*, 1983; Pask and Tomsia, 1988). Because of the important role played by the surface oxide layer, its structure, composition and morphology have been studied in some detail for a number of alloy systems submitted to thermal treatments (Ohno *et al.*, 1982, 1983; Mackert *et al.*, 1983; Hautaniemi *et al.*, 1990; Brantley *et al.*, 1993, 1995; Carr *et al.*, 1993). Changes in structure, morphology, composition and dis-

Table 1. Approximate composition (wt. %) of the alloys used in this investigation (provided by the manufacturers).

Alloy and Manufacturer	Alloying Elements									
	Au	Pd	Ag	Pt	Sn	In	Fe	Ga	Cu	Mn
Naturelle (Jeneric/Pentron)	2	79						9	10	
Jelstar (J.F. Jelenko & Co.)		60	28		6	6				
Acclaim (J. M. Ney Co.)		48.9	40.6			6.9				3.2
SMG-3 (J. M. Ney Co.)	81	11		6	1.1		0.8			

tribution of minor alloying elements in the surface layer on fusing with porcelain are critical in understanding the nature of interaction between the outermost oxide layer of the substrate and the opaque porcelain, but are not sufficiently investigated for many alloy systems. A satisfactory qualitative and quantitative description, comprising all aspects of the porcelain-alloy bond is still lacking. The purpose of this investigation was to characterize: (a) the morphology of the oxide layer on the metal substrate before firing of porcelain; (b) the morphology of the alloy/porcelain interface after the firing of porcelain; and (c) the distribution of oxidizable alloying elements in the vicinity of the interface of Pd-based and Pd-Ag alloys, and to compare these observations with results obtained for a high Au-content porcelain alloy. Furthermore, this investigation considered the mechanism for porcelain adhesion to Pd-base alloys containing different oxidizable elements and whether one unified mechanism for porcelain adhesion was operating with noble metal alloys.

Materials and Methods

Four alloy systems were investigated: a Pd-base alloy (Naturelle, Jeneric/Pentron, Wellingford, CT), two Pd-Ag alloys {Jelstar (J.F. Jelenko & Co., Armonk, NY) and Acclaim (J.M. Ney Co., Bloomfield, CT)} and a high Au-containing alloy (SMG-3; J.M. Ney). The alloy selection for this study was based on the desire to incorporate the alloys of widely different Pd and Ag contents as well as alloys with different kinds of minor oxidizable base metals. The detailed chemical compositions of the alloys (as provided by their manufacturers) are given in Table 1.

Four specimens for each alloy, measuring 20 mm long x 5 mm wide x 0.4 mm thick, were induction-melted, centrifugally-cast and prepared for porcelain bonding following manufacturers' recommendations. Following divesting, the specimens were air blasted with alumina (100 to 200 μm) and finished ground on 600 grit SiC abrasive paper to eliminate all traces of investment particles, surface oxides and other contaminants.

Table 2. Oxidation heat treatment procedure for the alloys tested.

Alloy	Procedure
Naturelle	650°C to 980°C at 55°C/min.; no vacuum, no hold
Jelstar	704° to 1038°C at 100°C/min.; no vacuum, no hold
Acclaim	650° to 1010°C at 55°C/min.; in vacuum, 5 min. hold
SMG-3	650° to 980°C at 32°C/min.; no vacuum, 10 min. hold

In order to prepare the surfaces for porcelain firing, the surfaces were air blasted with 50 μm alumina, cleaned by immersion in boiling water, and submitted to oxidation heat treatment (Table 2). One face from each specimen was overlaid with approximately a 0.2 mm thick opaque porcelain slurry and fired according to recommended temperature and time cycles as detailed in Table 3. Either one or two layers of opaque and one layer of body porcelains were fired.

A special specimen mounting technique was adopted to avoid a resin shrinkage gap and provide surface flatness with non-rounding of edges between the specimen and mounting resin. Two specimens with the oxide layer of one specimen facing the fused porcelain layer of other specimen were sandwiched under pressure with a c-clamp by a thin layer of special epoxy resin (Epo-Tek 353ND, Epoxy Technology Inc., Billerica, MA). After the thin layer was heat cured, the joined specimens were mounted in a conventional epoxy resin and ground and polished to a 0.05 μm diamond finish.

Scanning electron microscopy (SEM) (Cambridge, model 250 Mark II, Cambridge Instruments, Cambridge, UK), energy dispersive X-ray spectrometry (EDS) without light element detection capability, and digital EDS X-ray imaging techniques (IMIX-7, Princeton Gamma Tech, Princeton, NJ) were utilized to examine the cross-

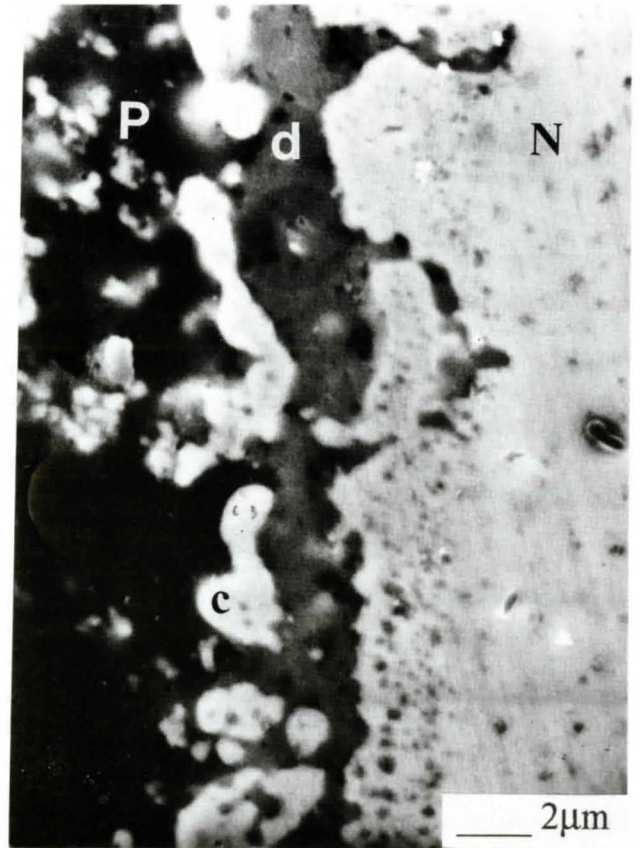
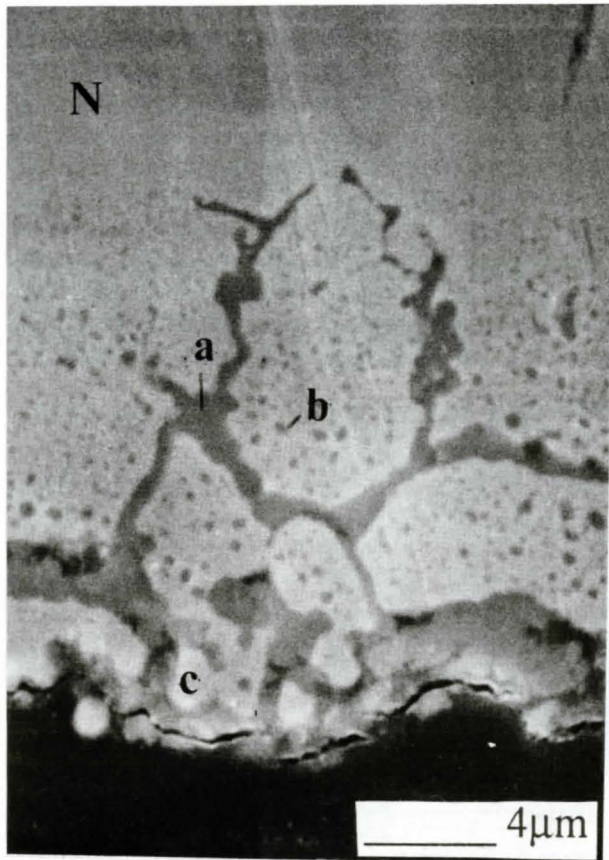


Figure 1 (at left). Near-surface microstructure of heat-treated Naturelle (N). No porcelain is present. Grain boundaries (a) and gray particles (b) contains mainly Ga and Cu.

Figure 2 (at right). Photomicrograph of a region of porcelain (P) fused to Naturelle (N) substrate showing Pd-Cu nodules (c) over Ga-Cu layer (d).

Table 3. Firing cycles for the opaque and body porcelains.

System	Low temp.	Hi-temp.	Rate	Vacuum	Remarks
Naturelle/Synspar					
Opaque	540°C	990°C	50°C/min.	yes	Release vac. at 890°C
Body	540°C	960°C	55°C/min.	yes	Release vac. at 890°C
Jelstar/Vita-VMK-68					
1st opaque	600°C	960°C	120°C/min.	yes	Release vac. at Hi-temp. and
2nd opaque	600°C	940°C	113°C/min.	yes	hold for 1 min.
Body	600°C	930°C	55°C/min.	yes	(for all firings)
Acclaim/Ceramco-II					
Opaque	650°C	970°C	70°C/min.	yes	Release vac. at Hi-temp., no hold
Body	650°C	940°C	70°C/min.	yes	Release vac. at 920°C, no hold
SMG-3/Ceramco					
Opaque	650°C	970°C	70°C/min.	yes	Release vac. at Hi-temp., no hold
Body	650°C	940°C	70°C/min.	yes	Release vac. at 920°C, no hold

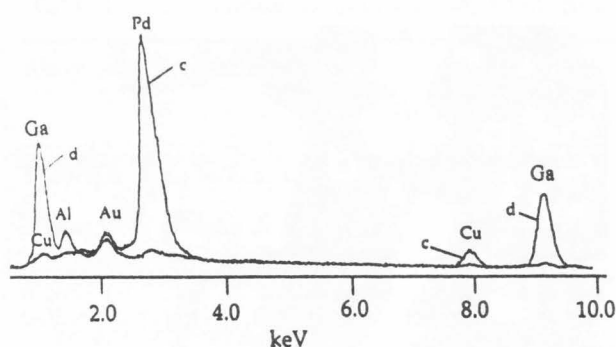


Figure 3. Typical EDS spectra of outer light nodular areas c in Figures 1 and 2 and of gray layer d in Figure 2. The Al peak is probably due to the embedded alumina particles from grit blasting of the alloy surface prior to oxidation heat treatment.

sections after the specimens were coated with either gold or carbon. The SEM was operated at an accelerating voltage of 20 kV. Secondary electron images were recorded and are presented here. Backscattered electron images were also investigated for detection of elemental distributions at the interface between porcelain and alloy. Further, digital X-ray maps of several elements were also generated simultaneously with EDS analysis.

Results

Naturelle (Pd-Cu-Ga)

Figures 1 and 2 present the scanning electron micrographs in cross-section of thermally treated (oxidized) alloy and the opaque porcelain fused to thermally treated alloy substrate respectively. The microstructure of the oxidized surface is characterized by the formation of (i) gray precipitates at the grain boundaries (a in Fig. 1), (ii) the gray particles (b in Fig. 1), (iii) the outermost light nodular areas (c in Fig. 2), and (iv) the near-surface light gray layer (d in Fig. 2). Within a depth of $\sim 15 \mu\text{m}$ below the surface of the sample, extensive precipitation in the grain interiors occurred. There was no specific size distribution of precipitated particles with distance from the surface. EDS spot analyses revealed that the gray precipitates (a in Fig. 1) and the gray particles (b in Fig. 1) contained mainly Ga and Cu.

EDS spectra for areas c (in Figs. 1 and 2) and d (in Fig. 2), presented in Figure 3, show that these areas contained mainly Pd and Cu, and Ga and Cu, respectively. These spot analyses were confirmed by digital X-ray maps for Pd, Cu and Ga in the thermally treated substrate (Fig. 4). These X-ray maps revealed that the external nodular areas were composed mainly of Pd with some Cu, and the underlying layer consisted of Ga and

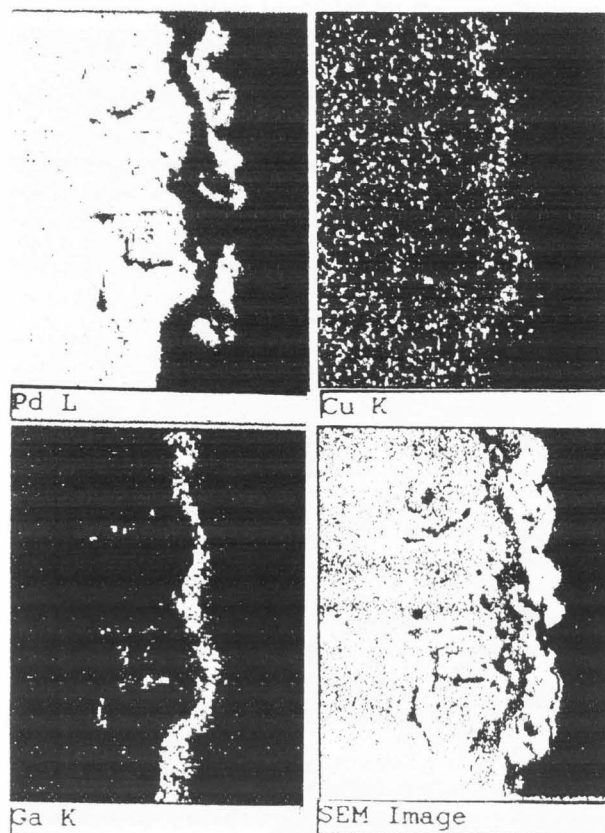


Figure 4. Scanning electron micrograph of heat-treated Naturelle and characteristic digital X-ray elemental maps of the same area formed by Pd(L α), Cu(K α) and Ga(K α).

Cu. Furthermore, the grain boundary precipitate was rich in Ga with some Cu. It was noted that after fusing the porcelain to the oxidized surface, the Pd-Cu nodules still existed (Fig. 2), but there were sections of the interface where such nodules were not present. EDS spot analyses at several locations in a region of porcelain lacking opaquing particles, showed the presence of Cu, Ga and Pd within $6 \mu\text{m}$ of porcelain. Cu diffused farthest, while Pd remained closer to the interface. Diffusion of Ga occurred only to short distances from the interface, but its concentration was highest.

Jelstar (Pd-Ag-Sn-In)

Figures 5 and 6 show scanning electron micrographs in cross-section of thermally treated (oxidized) alloy and of alloy/porcelain coupling. In many ways, the microstructure of the heat treated surface is different than the one with Naturelle. As before, internally precipitated particles occurred up to a depth of $\sim 12 \mu\text{m}$ from the surface. Figure 7 shows spectra from EDS spot analyses of nodular areas a (in Fig. 6) and particles f (in Figs. 5 and 6). The spectrum for layer h (in Fig. 5)

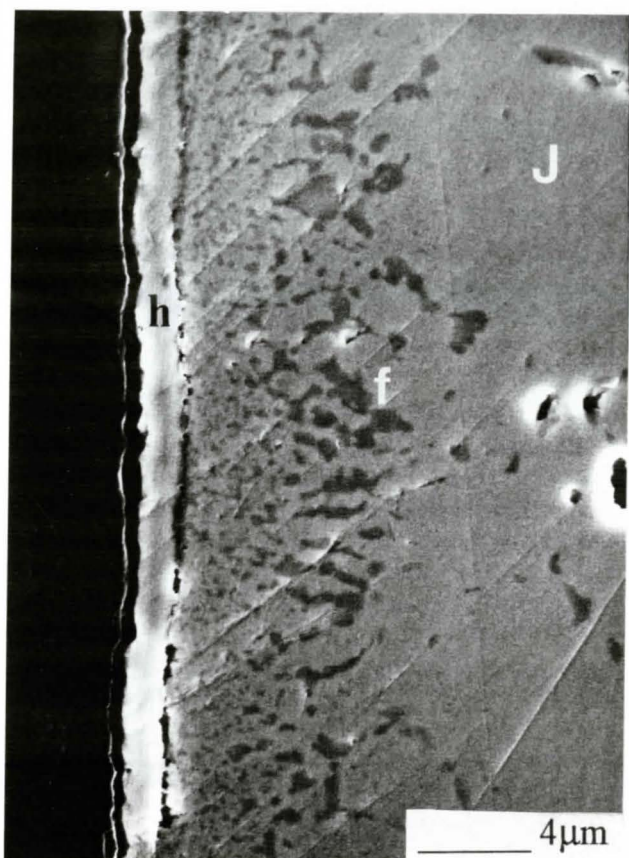


Figure 5. Detached outer layer (h) in Jelstar (J). The internally precipitated particles (f) are composed of mainly Sn with some In.

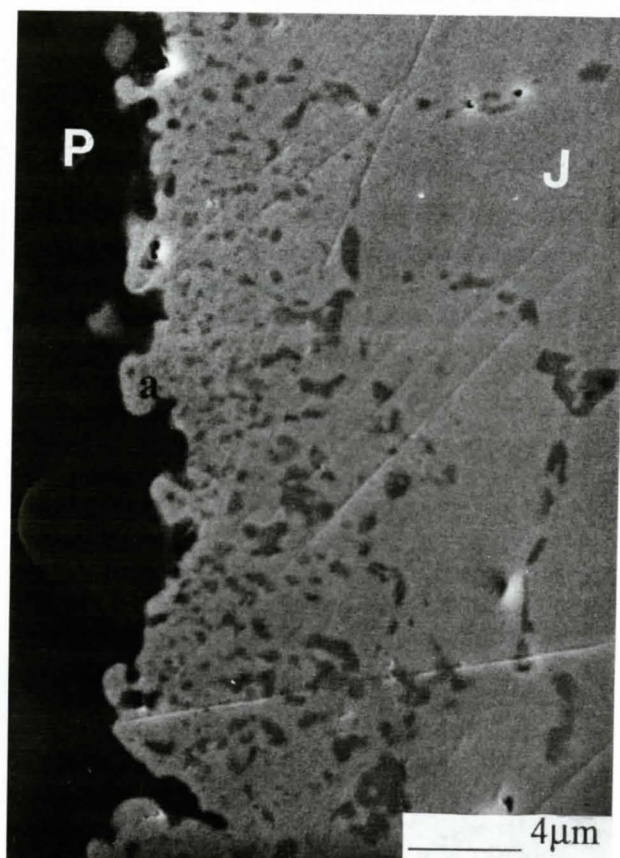


Figure 6. Typical micrograph of porcelain (P) fused to Jelstar (J) interface region. Nodules (a) in the interface regions are mainly of Ag-Pd.

was similar to that for nodules a (in Fig. 6) and is not being shown. The particles f (in Figs. 5 and 6) are rich in Sn and In, and their size tended to increase as the distance from the interface increased. This observation is similar to that reported with an alloy of the same elements (Mackert *et al.*, 1983) but with lower In (6% versus 1%) content. There is only one surface layer composed of predominantly Ag and Pd ($\sim 1.5 \mu\text{m}$; h in Fig. 5), formed by the thermal treatment. The EDS spectrum of this layer (not shown) failed to show the presence of Sn. Elemental X-ray mapping for elements Pd, Ag and Sn (Fig. 8) also indicated that the external layer was composed of Ag and Pd and the internally precipitated particles contained mainly Sn. The layer h (in Fig. 5) was often adherent to the surface, but occasionally a non-adherent layer, as shown in Figure 8, was also observed. The possibility existed that the surface layer was detached during specimen preparation. The continuity in the surface layer should have developed by coalescence of Ag-Pd nodules and, on firing porcelain, many of these nodules remained.

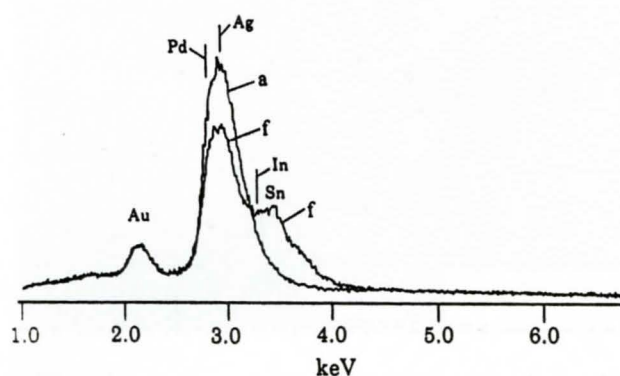


Figure 7. EDS spectra of light nodules (a in Fig. 6) at the porcelain/Jelstar interface and the gray particles (f in Fig. 5) in the interior. The spectra of from areas a (in Fig. 6) and h (in Fig. 5) were similar.

Acclaim (Pd-Ag-In-Mn)

This alloy system is similar to Jelstar, except that Sn in Jelstar is replaced by Mn and the percentage of Pd in

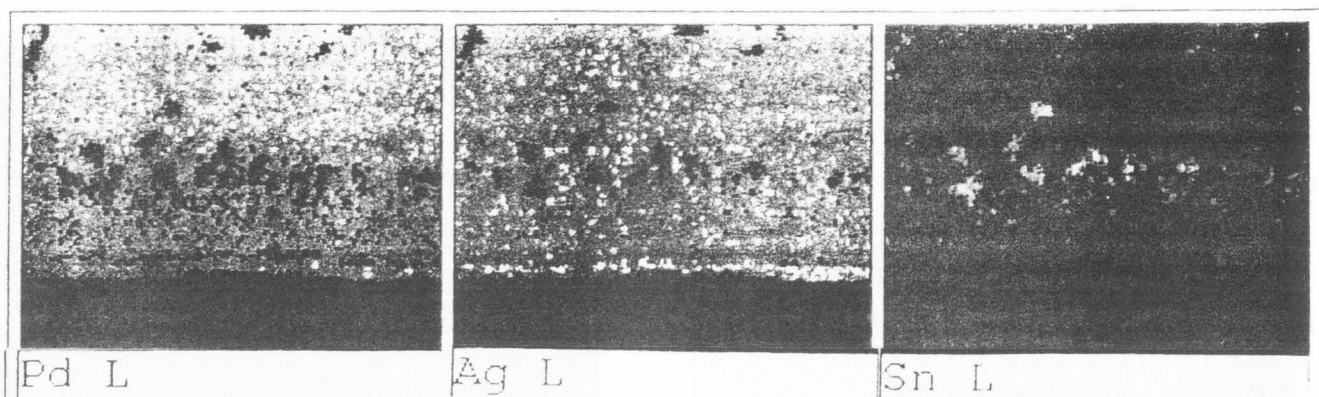


Figure 8. Characteristic digital X-ray elemental maps of heat-treated Jelstar surface formed by Pd(L α), Ag(L α), and Sn(L α).

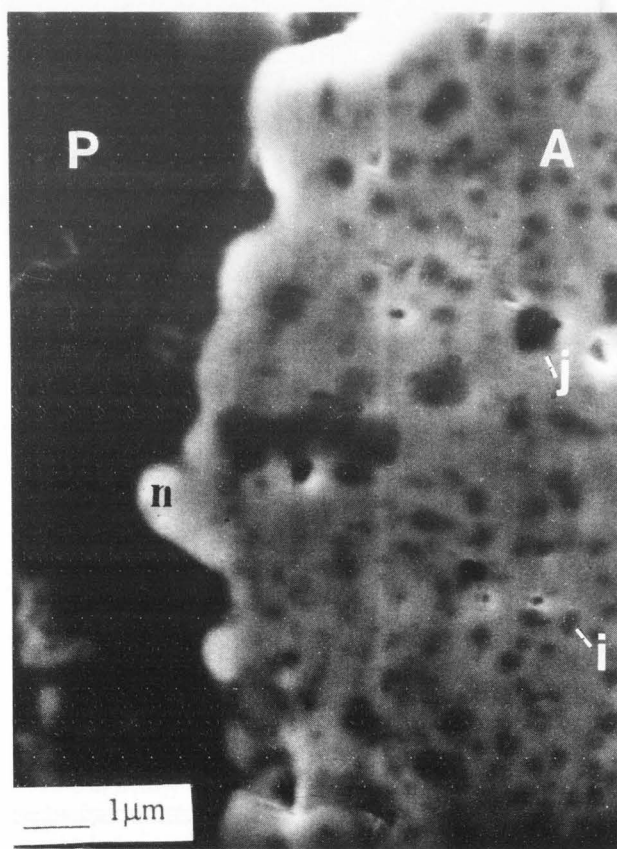


Figure 9. Interfacial microstructure of porcelain (P) / Acclaim (A) coupling showing precipitated particles (i and j) containing base metals and Ag-Pd nodules (n) at the interface.

Jelstar is reduced in Acclaim by an increase in Ag. The Acclaim alloy contains less than 50 wt. % Pd. The microstructure of the heat-treated alloy surface was similar to that seen in Jelstar. The surface layer was always adherent to the metal and had the appearance of coalesced

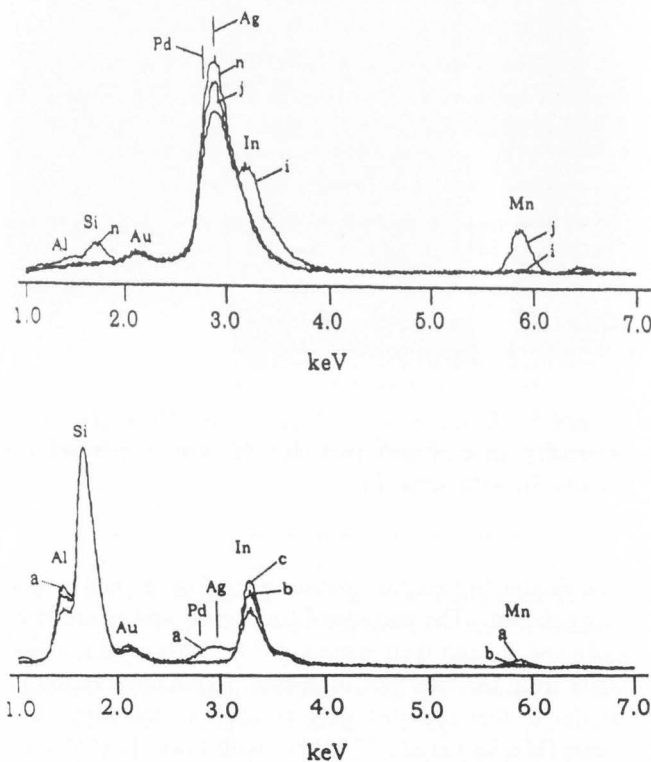


Figure 10. Typical EDS spectra of nodular area (n in Fig. 9) at the interface, and the internally precipitated particles (i and j in Fig. 9).

Figure 11. EDS spot spectra in a clearer matrix of porcelain as a function of distance from the porcelain/Acclaim interface. In was detected at a distance up to $\sim 4 \mu\text{m}$ from the interface. Locations (in porcelain from the interface): a at $\sim 1 \mu\text{m}$; b at $\sim 2 \mu\text{m}$; and c at $\sim 4 \mu\text{m}$.

Ag-Pd nodules. An extensive internal precipitation of particles containing minor alloying elements, Mn and In, occurred within about $\sim 12 \mu\text{m}$ from the surface (Fig. 9). Unlike Jelstar, the average size of these particles did

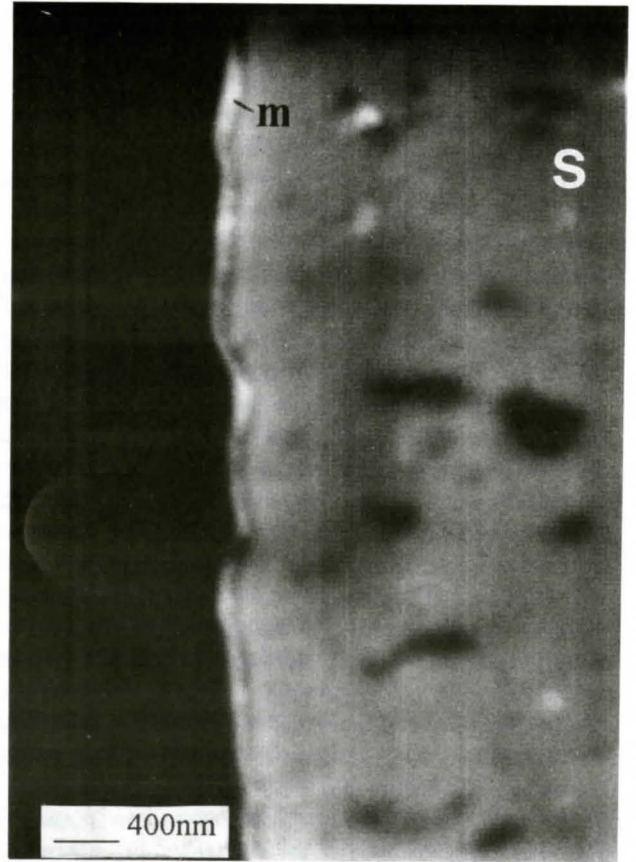
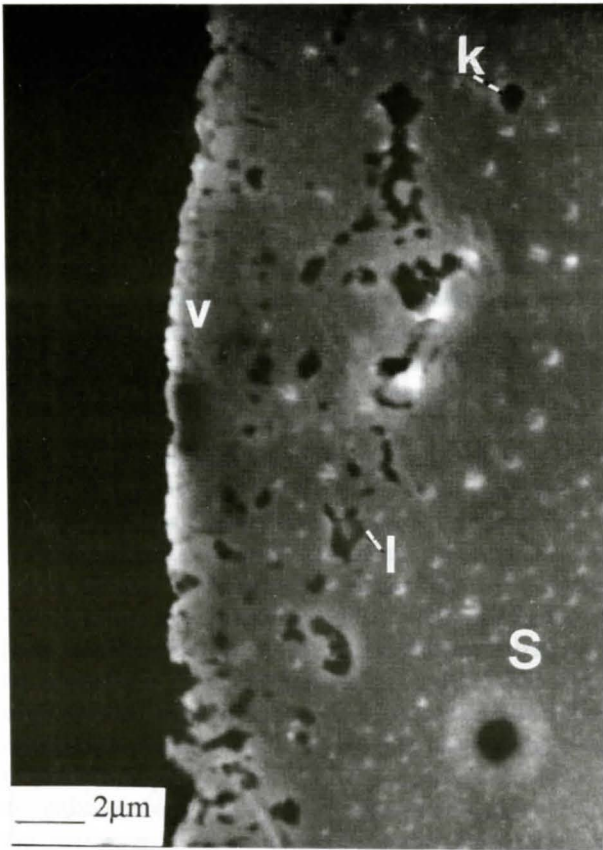


Figure 12 (at left). Photomicrograph of near-surface areas of heat treated SMG-3. The microstructure consists of internally precipitated particles (such as at k and l) and the thin surface layer of coalesced tiny nodules (at v).

Figure 13 (at right). Micrograph of the surface of heat-treated SMG-3, showing a very thin (~100 nm) outermost layer containing Fe, Sn and Pd.

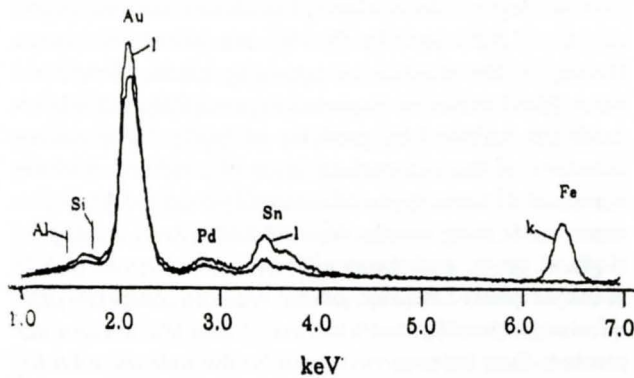


Figure 14. Typical EDS spot spectra of particles k and l (in Fig. 12).

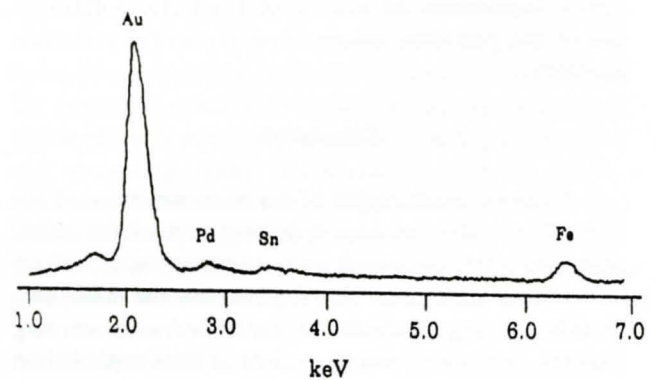


Figure 15. EDS spot spectrum of thin surface layer m (in Fig. 13). It is richer in Fe and Sn than the bulk.

not change with distance from the interface. Further, these precipitated particles had different shades of gray. The darkest gray particles (j in Fig. 9) contained mostly Mn while the lightest gray particles (i in Fig. 9) contained mostly In (Figs. 9 and 10). The particles of in-between shades contained both Mn and In. The alloy/

porcelain interface microstructure was similar to the Jelstar/porcelain interface. After porcelain firing, several Ag-Pd nodules (n in Fig. 9) still remained at the interface. In addition, In and Mn were detected at a distance up to ~4 μm in the porcelain from the oxide/porcelain interface (Fig. 11). Pd and Ag were also present in the

porcelain but always closer to the interface, and In diffused farther than Mn into the porcelain from the interface.

SMG-3 (Au-Pd-Pt-Sn-Fe)

This is a high Au (~80%)-Pd alloy. Figures 12 and 13 present scanning electron micrographs in cross-section of heat-treated surfaces. The morphologies of the heat-treated substrate and the alloy/porcelain interface (micrograph not shown) were similar to Jelstar and Acclaim, even though the extent of changes differ from material to material. There was an internal precipitation of base metals Sn and Fe in the surface layer, which was usually less than ~8 μm from the surface. The EDS spot analyses (Fig. 14) indicated that the dark-gray particles (k in Fig. 12) are rich in Fe while the light-gray particles (l in Fig. 12) are rich in Sn. The thickness (100 nm - 2 μm) of the outermost surface layer varied with location and in some other characteristics. In some regions, this layer gave the appearance of the coalescence of very tiny surface nodules (v in Fig. 12). It was usually adherent to the surface as in Jelstar and Acclaim. At some locations, this layer was extremely thin (100 nm; m in Fig. 13) and often disappeared on long exposure to the electron beam in the SEM. Furthermore, this outermost layer was found to contain Fe, Sn and Pd (Fig. 15). Occasionally, a thick detached layer, similar to the one seen in Jelstar, was also detected (micrograph not shown). The morphological characteristics at the alloy/porcelain interface were similar to those for the two Pd-Ag alloys examined. The projecting nodular areas in porcelain had a similar composition to the outer layer. In addition, Sn and Pd were detected within ~1 μm of the porcelain matrix from the oxide/porcelain interface.

Discussion

A careful examination of the microstructures of the four alloys after the heat treatment and of the alloy/porcelain interfaces reveal many common features along with some differences. This suggests that the minor oxidizable alloying elements act similarly but to varying degrees. It is likely that the extent of their contribution in modifying the surface layer bonding depends upon alloy composition and initial oxidation heat-treatment. Even though a light-element detector was not used (and therefore, the presence of oxygen could not be confirmed), there are numerous studies indicating that these minor elements form oxides on heat treatment. Based on these studies, it is summarized that there was internal oxidation of Ga and Cu in Naturelle, Sn and In in Jelstar, In and Mn in Acclaim, and Sn and Fe in SMG-3. The following oxide particles were formed: $\text{Ga}_2\text{O}_3\cdot\text{CuO}$

spinel (Kingery *et al.*, 1976; Cascone, 1983; Suoninen and Hero, 1985; Hautaniemi *et al.*, 1990; Brantley *et al.*, 1996) in Naturelle; SnO_2 and In_2O_3 (Ohno *et al.*, 1982, 1983; Mackert *et al.*, 1983) in Jelstar; In_2O_3 (Ohno *et al.*, 1982, 1983) and MnO or Mn_2O_3 in Acclaim; and SnO_2 and Fe_2O_3 in SMG-3 (Ohno *et al.*, 1982; Ohno and Kanzawa, 1983). Further, the observations on differently shaded particles in scanning electron micrographs of Jelstar, Acclaim and SMG-3, and the difference in their respective EDS spectra, reveal that, in these alloy systems, the ratio of the two oxides in the particles is not the same. A mixed (A,B)O oxide may precipitate as internal oxides in an A-B type alloy if oxides AO and BO have considerable mutual solubility, since such a process would lower the free energy of the system.

In noble alloys containing base metals, the standard free energy of formation (ΔG°) of an oxide, the concentration (c) of the base metal in the alloy, and the metal/oxygen atomic ratio (u/v) in the oxide are useful parameters in determining the oxidation tendency of base metal constituents (Ohno and Kanzawa, 1983). A metal with higher $-\Delta G^\circ$, c and u/v has an increased driving force for oxidation and is preferentially oxidized. The Gibbs' standard free energy ($-\Delta G^\circ \cdot \text{Kcal/mol}^{-1} \text{O}_2$ at 1223K) of formation of the oxides (Klar, 1987), in decreasing order, are listed below followed by their respective u/v ratio: MnO (137.3, 1) > Ga_2O_3 (109.2, 0.67) > FeO (85, 1) > In_2O_3 (84.5, 0.67) > SnO_2 (77.2, 0.5) > Fe_2O_3 (76.7, 0.67) > Cu_2O (38.3, 2) > CuO (22.9, 1) > PdO (-2, 10) > Au_2O_3 (-41, 0.67). Both, the value of $-\Delta G^\circ$ and the atomic ratio u/v, for MnO are higher than for In_2O_3 . In Acclaim, the atomic concentrations of Mn (7.8%) and In (8.0%) are about the same. Hence, in the absence of opposing kinetic considerations, MnO would be expected to precipitate initially on oxidation followed by particles of In_2O_3 . The microstructure of the sub-surface layer of oxidized Acclaim consisted of three types of internally oxidized particles: those containing mostly Mn (darkest gray), mostly In (lightest gray), and those with Mn in the center and In at the periphery. Besides thermodynamic considerations, microstructures due to oxidation of base metals also depend on their heterogeneity and on the pathways for O_2 diffusion. The grain boundaries are easier pathways for O_2 diffusion, and the base metals to be oxidized were preferentially distributed at the grain boundaries and the interdendritic areas. In the present alloys containing two or more base metals, a continuous change occurred in the ratio of atomic concentration of base metals in localized areas as the preferential base metal oxidized, thus, altering the parameters in favor for oxidation of the second base metals.

In the case of Jelstar, $-\Delta G^\circ$ and u/v are similar for

In_2O_3 and SnO_2 , and the atomic concentrations of In (5.6%) and Sn (5.4%) are about the same. Under these circumstances, both elements oxidized simultaneously. For SMG-3, both $-\Delta G^\circ$ and the atomic ratio u/v for FeO are higher than for SnO_2 . The atomic concentration of Fe (2.5%) is greater than Sn (1.6%). For these reasons, Fe preferentially oxidized in the interior, but, as for Acclaim, some particles here predominantly contained one base metal (Fe, darkest gray) while the others contained mostly the second base metal (Sn, lighter gray). For Naturelle, a more complicated situation exists. The atomic concentrations of both base metals, Ga (12.4%) and Cu (15.1%), are large and about the same. The standard free energy change for Ga_2O_3 formation is significantly larger than for Cu_2O , but the u/v ratio for Ga_2O_3 is smaller than for Cu_2O . The data do not predict the specific oxide that forms preferentially. However, examination of the microstructure of oxidized Naturelle showed an externally oxidized layer of Ga-rich Ga-Cu beneath the outermost layer of Pd-Cu nodules, grain boundary oxides of Ga-rich Ga-Cu, and oxide particles of Ga-poor Ga-Cu within grain interiors. This suggests that besides the free energy considerations, the microstructure of oxidized Naturelle was strongly influenced by the heterogeneity of its cast structure.

Pd-based and Pd-Ag alloy systems revealed an outermost layer of Pd-containing nodules which formed during the initial heat treatment. The nodules were primarily composed of Pd and Cu in Naturelle, and of Ag and Pd in Jelstar and Acclaim. To a lesser degree, Pd-containing nodules with Fe and Sn also formed in SMG-3. In areas where the oxidation was extensive, nodules coalesced and formed a continuous outermost layer which was generally adherent, although it is possible that the surface layer occasionally became detached during the specimen preparation. However, when the porcelain is fired on the oxidized alloy surface, the fused porcelain makes contact with the continuous coalesced nodular layer or the alloy nodules and the alloy surface between the nodules. The presence of a nodular morphology at the alloy/porcelain interface in all of these alloy systems, and the EDS spectra of these nodules, suggest that the surface layer fuses and often partially survives the porcelain firing, and becomes part of an interface zone in the alloy/porcelain coupling. Ag in the outer layer should not be in the form of oxide as it has been shown that the Ag_2O is thermodynamically unstable above 146°C in air (Wodniecki and Wodniecka, 1982). Further, PdO is considered to be unstable for the heat treatment cycle used in this investigation (Mackert *et al.*, 1983). However, Brantley *et al.* (1996) detected Pd oxide in varying amounts by X-ray diffraction and X-ray photoelectron spectroscopy in Pd-Cu-Ga alloys when subjected to oxidation heat treatment.

The characteristics of the oxide layer in Jelstar are basically similar to those seen in a study of Will-Ceram W1 (Mackert *et al.*, 1983), which has a similar wt. % of Pd, Ag and Sn but very little In. In both alloy systems, there were internally oxidized particles, and their diameter tended to increase as the distance from the interface increased. However, no such change in size of internally oxidized particles was noted in Naturelle, Acclaim and SMG-3. Mackert *et al.* (1983) were able to explain the formation of metallic binary Pd-Ag nodules on the surface of the Pd-Ag-Sn-In alloy by a Nabarro-Herring diffusion creep mechanism which was driven by the increased volume of oxide formed by the internal oxidation of Sn and In. The increased molar volume for Sn on oxidation was 60% while for In it was 48%. Further, Mackert *et al.* (1983) showed that the volume increase of Sn and In due to internal oxidation was equal to the volume of nodules formed on the surface. A similar calculation shows that the internal oxidation of Cu to Cu_2O , Ga to Ga_2O_3 , Mn to MnO and Mn_2O_3 , and Fe to FeO and Fe_2O_3 also gives rise to a large increase in molar volume, of the order of 72%, 91%, 172% and 267%, and 85% and 127%, respectively. Thus, like Sn and In in Will-Ceram W1 and Jelstar, the internal oxidation of Cu, Ga, Mn and Fe will also generate hydrostatic stresses to operate a Nabarro-Herring diffusional creep mechanism in the alloy systems investigated here and form nodules on the surface during oxidation heat treatment.

Other morphological features of the oxidized surfaces in the other alloy systems do not coincide with oxidized features of Jelstar. For example, there is no size dependency of internally oxidized particles with distance from the surface. In Naturelle, there is an intermediate layer of mixed oxides of Ga and Cu sandwiched between the outermost nodular Pd-Cu and the internally oxidized region (Figs. 2 and 4) and massively thick grain boundaries containing oxides of Ga and Cu (Figs. 1 and 4). Naturelle, more so than the other alloys studied, contains a relatively higher base metal concentration. The formation of an intermediate layer and grain boundary precipitate may qualitatively be understood as follows. The cast structure of Pd-Cu-Ga alloys was observed to be heterogeneous with segregation of Cu and Ga into interdendritic and grain boundary areas (Oden and Hero, 1986; Brantley *et al.*, 1993). Oxygen diffused rapidly in the Pd lattice (solubility of O_2 is greater in Pd). At relatively low temperatures, the internal oxidation may proceed faster along grain boundaries, as these are easier pathways for O_2 diffusion. At higher temperatures, oxygen diffused more rapidly into the Pd lattice and internally oxidized the interdendritic Ga-Cu rich areas into discrete particles of Ga-Cu mixed oxides. As mentioned earlier, this process formed a layer of Pd-Cu nodules on

the surface by the Nabarro-Herring diffusional creep mechanism. Further, it has been seen in some alloy systems that when the mole fraction of the less noble metal is increased to exceed a certain critical value, the alloy no longer oxidizes internally but rather forms an oxide layer of the less noble metal on the outer surface (Rapp, 1961). Wagner (1959) proposed a theory in which it was assumed that the transition from internal to external oxidation is caused by the blocking of the diffusion processes upon the formation of a critical volume percent of the internal oxide in the matrix. The composition of Naturelle is such that both internal and external oxidation take place. The formation of Pd-Cu nodules on the surface will increase the mole fraction of Ga in the interior. Sufficient O_2 at the interface was still available because of the high permeability of O_2 in the Pd-Cu nodules and open regions between nodules. Both of these conditions led to a transition from internal oxidation to external oxidation, thus, forming a Ga-Cu oxide layer beneath Pd-Cu nodules.

In pure gold, the solubility of O_2 is very small (below 2×10^{-5} at. %; Eichenauer and Muller, 1992). Therefore, no extensive internal oxidation of alloys based on Au is expected, even though the presence of Pd and Ag in the gold alloy might increase the solubility of O_2 . The SEM examination of oxidized SMG-3 showed discrete oxide particles of Fe and Sn in a narrow surface zone ($\sim 8 \mu\text{m}$; Fig. 15). This oxidized zone is comparatively small, but most of its characteristics are similar to the internally oxidized regions of other alloy systems investigated. The occasional appearance of tiny nodules containing Pd, Sn and Fe on the surface may again be the result of a limited operation of the Nabarro-Herring creep mechanism due to limited internal oxidation in near-surface regions. However, the important feature here was the presence of a very thin oxide film rich in Fe and Sn. This alloy contained only a small amount of Fe and Sn, and the availability of these elements for surface oxidation is further reduced by internal oxidation. Therefore, only a very thin oxide film is to be expected. On an alloy of similar composition, Ohno *et al.* (1982) have identified, by X-ray diffraction and electron probe microanalysis, that the external oxide layer is composed of Fe_2O_3 over an internal layer of SnO_2 . In our alloy system, we did not notice two distinct layers of different oxides, but rather one layer containing both oxides.

Sometimes, a thick non-adherent outer layer formed in Jelstar (Fig. 5) and SMG-3. The variability in film thickness and other morphological characteristics may be the result of uneven surface treatment such as alumina blasting before the oxidation heat treatment. In the case of Jelstar, the detached outer layer was solely composed of coalesced Pd-Ag nodules, while in SMG-3, this layer

contained all the alloying elements with increased Fe and Sn. The mechanism of detachment is not clear, but one can envision a process where vacancies annihilate at the interface, thus, creating voids and detachment of the film. The possibility of detachment during metallographic preparation of specimen also existed. Further, the microstructure at the alloy/porcelain interface in all alloy systems studied appear similar. The outer oxidized surface layer of the alloy became non-uniform and rounded when contacted with fused porcelain. The EDS spectra of these projected rounded regions in porcelain are similar to the EDS spectra of the oxidized surface layer of the alloy. These suggested that when porcelain is fired onto the oxidized surface, partial softening/melting of high energy regions, such as, corners of the outermost surface layer of the substrate, must occur. The surface tension and the viscosity of the fused material at the interface also were important in generating the observed interfacial microstructures. The partial melting of the surface layer and the presence of fused porcelain in the vicinity at the interface would create an intimate interaction between the two materials. The fused viscous porcelain must have infiltrated spaces at the partially melted substrate and between the surface nodules, and, at the same time, metal cations from the viscous outermost layer of the substrate diffused further into the fused porcelain matrix.

If the interface morphology formed as described, then, several factors should contribute to the bond between alloy and the porcelain. Mechanical bonding definitely formed when fused porcelain occupied areas in-between the surface nodules as suggested by Mackert *et al.* (1983) and areas in the partially melted outer layer of the substrate. This may be the predominant component of the bond in the case of the Jelstar and Acclaim alloy systems. But, since fused porcelain makes significant contact with gallium copper oxide spinel ($Ga_2O_3 \cdot CuO$) in Naturelle, and with the Fe_2O_3 - SnO_2 layer in SMG-3, the chemical bonding as formulated in the "oxide interface theory" (King *et al.*, 1959; Pask and Fulrath, 1962) must be an important contributing factor to the alloy/porcelain bond in these two alloy systems.

Conclusions

(1) The outer $\sim 15 \mu\text{m}$ layer of Naturelle was characterized by the presence of internally oxidized Ga-Cu particles, grain boundary precipitation of Ga-Cu oxides and a Ga-Cu rich layer beneath the Pd-Cu surface nodules. On firing porcelain, diffusion of Cu, Ga, and Pd occurred into the porcelain within a distance of $\sim 6 \mu\text{m}$.

(2) Extensive internal oxidation of minor alloying elements, Sn and In, and In and Mn, also occurred within $\sim 12 \mu\text{m}$ of surface layer of Jelstar and Acclaim,

respectively. The average size of oxidized particles in Jelstar tended to increase as the distance from the surface was increased. However, such a relationship did not exist with Acclaim. Both of these alloys revealed a thin surface layer of coalesced Ag-Pd nodules. Further, Pd and Ag were detected in close proximity of the interface with fired porcelain, while In and Mn diffused to greater distances.

(3) The thermal treatment of SMG-3 also revealed an internal oxidation of base metals Sn and Fe in a surface layer which was usually less than $\sim 8 \mu\text{m}$ wide. The surface oxide layer varied in thickness from 100 nm to $2 \mu\text{m}$ and contained Fe, Sn and Pd.

(4) The morphological characteristics at the alloy/porcelain interface appeared similar in all alloy systems.

(5) The predominant mechanism of adherence for alloy/porcelain coupling in Jelstar and Acclaim alloy systems is a mechanical bond formation, while for Naturelle and SMG-3 alloy systems, a significant component of chemical bonding appeared to be present.

Acknowledgment

Support was provided by NIH contract No 1-DE-12584.

References

Anusavice KJ (1985) Noble metal alloys for metal-ceramic restorations. *Dent Clin No Amer Ceramics* 29(4), 789-803.

Anusavice KJ, Horner JA, Fairhurst CW (1977) Adherence controlling elements in ceramic-metal systems I. Precious alloys. *J Dent Res* 56, 1045-1061.

Baran GR (1985) Selection criteria for base metal alloys for use with porcelains. *Dent Clin No Amer Ceramics* 29(4), 779-787.

Borom MP, Pask JA (1966) Role of adherence oxides in the development of chemical bonding at glass metal interfaces. *J Am Ceram Soc* 49, 1-6.

Brantley WA, Cai Z, Carr AB, Mitchell JC (1993) Metallurgical structure of as cast and heat-treated high-palladium alloys. *Cells Mater* 3, 103-114.

Brantley WA, Cai Z, Papazoglou, E, Mitchell JC, Kerber SJ, Mann GP, Barr TL (1996) X-ray diffraction studies of oxidized high-palladium alloys. *Dent Mater* 12, 333-341.

Carr AB, Cai Z, Brantley WA, Mitchell JC (1993) New high-palladium casting alloys: Part 2. Effects of heat treatment and burnout temperature. *Int J Prosthodont* 6, 233-241.

Cascone PJ (1983) Oxide formation and palladium alloys and its effect on porcelain adherence. *J Dent Res* 62 (spec issue), 255 (AADR Abstract #772).

Eichenauer VW, Muller G (1962) Diffusion und Löslichkeit von Sauerstoff in Silber (Diffusion and solubility of oxygen in silver). *Z Metallk* 53, 321-324.

Fairhurst CW (1977) Metal surface preparation and bonding agents in porcelain-metal systems. In: *Alternatives to Gold Alloys in Dentistry*. Valega TE (ed.). Natl. Inst. Health, Dept. Health Education and Welfare Publication #NIH77-1227, Bethesda, MD. pp. 255-274.

Fairhurst CW, Mackert Jr. JR, Twigg SW, Ringle RD, Hashinger DT, Parry EE (1985) Bonding of ceramics to alloys. In: *Proc. Conf. Recent Developments in Dental Ceramics*. O'Brien WJ, Craig RG (eds.). The American Ceramic Society, Columbus, OH. pp. 66-83.

Hautaniemi JA, Juhanoja JT, Suoninen, Yli-urpo AUO (1990) Oxidation of four palladium rich ceramic fusing alloys. *Biomaterials* 11, 62-72.

King BW, Tripp HP, Duckworth WH (1959) Nature of adherence of porcelain enamels to metals. *J Am Ceram Soc* 42, 504-525.

Kingery WD, Bowen HK, Uhlmann DR (1976) *Introduction to Ceramics*, 2nd ed. Wiley, New York. pp. 61-70.

Klar E (1987) Chemical methods of powder production. In: *Metals Handbook*, 9th ed., vol. 7. American Society for Metals, Metals Park, OH. p. 53.

Laub LW, Marshall GW, Lautenschlager EP, Eichner K (1978) The metal-porcelain interface of gold crowns. *J Dent Res* 57 (special issue A), 293 (IADR Abstract #874).

Lautenschlager EP, Greener EH, Elkington WE (1969) Microprobe analyses of gold-porcelain bonding. *J Dent Res* 48, 1206-1210.

Mackert JR Jr, Ringle RD, Fairhurst CW (1983) High temperature behavior of a Pd-Ag alloy for porcelain. *J Dent Res* 62, 1229-1235.

Mackert JR Jr, Parry EE, Hashinger DT, Fairhurst CW (1984) Measurements of oxide adherence to PFM alloys. *J Dent Res* 63, 1335-1340.

Mackert JR Jr, Ringle RD, Parry EE, Evans AL, Fairhurst CW (1988) The relationship between oxide adherence and porcelain metal bonding. *J Dent Res* 67, 474-478.

Miyagawa Y (1978) X-ray diffraction at the metal-ceramic interface Part I. Commercial gold alloys-porcelain interface. *Nippon Dent Univ Annu Pub* 12, 57-61.

Nally JN (1968) Chemico-physical analysis and mechanical tests of the ceramo-metallic complex. *Int Dent J* 18, 309-325.

O'Connor RP, Mackert JR Jr, Myers ML, Parry EE (1996) Castability, opaque masking and porcelain bonding of 17 porcelain-fused-to-metal alloys. *J Prosthet Dent* 75, 367-374.

Oden A, Hero H (1986) The relationship between hardness and structure of Pd-Cu-Ga alloys. *J Dent Res*

65, 75-79.

Ohno H, Kanzawa Y (1983) Internal oxidation of gold alloys containing small amounts of Fe and Sn. *J Mater Sci* 18, 919-929

Ohno H, Ichikawa T, Shiokawa N, Ino S, Iwasaki H (1981) ESCA study on the mechanism of adherence of metal to silica glass. *J Mater Sci* 16, 1381-1390.

Ohno H, Miyakawa O, Watanabe K, Shiokawa N. (1982) The structure of oxide formed by high-temperature oxidation of commercial gold alloys for porcelain-metal bonding. *J Dent Res* 61, 1255-1262.

Ohno H, Kanzawa Y, Kawashima I, Shiokawa N (1983) Structure of high-temperature oxidation zones of gold alloys for metal-porcelain bonding containing small amount of In and Sn. *J Dent Res* 62, 774-779.

Pask JA (1977) Fundamentals of wetting and bonding between ceramics and metals. In: *Alternatives to Gold Alloys in Dentistry*. Valega TE (ed.). Natl. Inst. Health, Dept. Health Education and Welfare Publication #NIH77-1227, Bethesda, MD. pp. 235-254.

Pask JA, Fulrath RM (1962) Fundamentals of glass-to-metal bonding: VIII. Nature of wetting and adherence. *J Am Ceram Soc* 45, 592-596.

Pask JA, Tomsia AP (1988) Oxidation and ceramic coatings on 80Ni 20Cr alloys. *J Dent Res* 67, 1164-1171.

Rapp RA (1961) The transition from internal oxidation to external oxidation and the formation of interruption bands in silver-indium alloys. *Acta Met* 9, 730-741.

Sarkar NK, Verret M, Eyer CS, Jeanson EE (1985) Role of gallium in alloy-porcelain bonding. *J Prosthet Dent* 53, 190-194.

Stewart GP, Maroso D, Schmidt JR (1978) Topography and distribution of trace metals (Sn, In) on alloys for porcelain-metal restorations: Influence of surface treatments. *J Dent Res* 57, 237-243.

Suoninen E, Hero H (1985) The structure and oxidation of two palladium ceramic fusing alloys. *Biomaterials* 6, 133-137.

Tomsia AP, Pask JA (1986) Chemical reactions and adherence at glass/metal interface: An analysis. *Dent Mater* 2, 10-16.

von Radnoth, Szantho M, Lautenschlager EP (1969) Metal surface changes during porcelain firing. *J Dent Res* 48, 321-324.

Vrijhoef MMA, van Der Zel JM (1988) Oxidation of a gold-palladium PFM alloy. *J Oral Rehab* 15, 307-312.

Wagner C (1959) Reaktionstypen bei der oxidation von Legierungen (Types of reaction in the oxidation of alloys). *Z Electrochem* 63, 772-790.

Wodniecki P, Wodniecka B (1982) TDPAC studies of internal AgIn alloy oxidation. *Hyper Inter* 12, 95-104.

Zacky VF, Mitchell DW, Mitoff SP, Pask JA (1953) Fundamentals of glass-to-metal bonding: 1. Wettability of some group I and group VIII metals to sodium silicate glass. *J Am Ceram Soc* 36, 84-89.

Discussion with Reviewers

W.A. Brantley: Our research with two alloys of nominally identical composition (Spartan and Spartan Plus, Williams/Ivoclar) suggest that the Pd-Cu-Ga alloy Naturelle has a dendritic as-cast microstructure. What differences would this type of microstructure contribute to the porcelain-metal interaction compared to a noble alloy with an equiaxed fine-grained microstructure? What type of as cast microstructure was found for Jelstar, Acclaim and SMG-3? What was the effect of the porcelain-firing heat treatment on the four as-cast alloy microstructures?

Authors: Although our micrographs show the alloy surfaces away from the porcelain/alloy interface, our studies did not examine as-cast microstructures. It is not known if the alloy's degassing and porcelain firing heat treatments modified as-cast structures. It is expected the heat treatments, for short times and at temperatures several hundred degrees below the alloy's melting temperatures, for both dendritic and equiaxed fine-grained cast structures caused some microstructural homogenization, even if only on the surface by diffusion. Intuitively, it is expected that as-cast dendritic structures are modified more than equiaxed structures due to the former's greater departure from equilibrium conditions. Porcelain bonding should be more favorable with the cast dendritic structure, since: (1) this surface is at a higher energy; (2) it contains regions with greater compositional differences and a better chance to chemically interact; and (3) it often contains enhanced microstructural features for mechanical bonding.

Although microstructural considerations are important, it is the authors' contention that the techniques in preparing and altering an alloy's surface prior to, between, and after heat treatments are more important in affecting porcelain fused to metal bond (Mueller, 1996). Surface preparation affects composition of the oxide and the rate of oxidation. Numerous variations in preparation exist. Some of these include grit grinding and air abrasion with alumina and other particles. Alteration in surface properties is very convenient with air abrasion technology and offers numerous possibilities to enhance both chemical and mechanical porcelain fused to metal bonding. Since the surfaces are transformed into material different from that of the as-cast structure, emphasis should also be placed on surface modification techniques instead of totally on the cast microstructures and their modifications due to porcelain processing. Air abrasion

technology offers the possibility of forming distinct surface films or layers on alloy surfaces which de-emphasizes base metal content of substrate and its microstructure.

W.A. Brantley: The authors discuss the oxidation tendencies of the base metal elements in these noble alloys in terms of the Gibbs standard free energy of formation for the oxide species, as well as the metal/oxygen ratio for the oxides. The multicomponent alloy compositions and the reduced atmospheric pressure result in non-standard state conditions during oxidation, and there may be additional kinetic effects associated with the oxide formation. Can the authors comment on the potential consequences of these effects for their model?

Authors: The free energy changes presented are standard free energy changes for the pure metal oxides from the pure metals and oxygen at 1 atmosphere (atm.). An equation of the type $M(s) + O_2(g) = MO_2(s)$ is represented by an equilibrium constant $K = 1/p_{O_2}$. This reveals that for many of the metals considered, oxidation at 1000°C proceeds if p_{O_2} is greater than 10^{-7} to 10^{-26} atm. Hence, even if the partial pressure of oxygen in air during firing was lowered sufficiently, external oxidation still occurred spontaneously. A comparison of these data also has merit for the multicomponent alloys. Comparison of the magnitudes of the free energy changes for pure metals in contact reveals the metals to be oxidized (more negative free energy change) and those metal oxides to be reduced. Alloy microstructure has an effect upon these tendencies. Localized concentrations and distribution of the different metals can kinetically alter the oxidation tendencies. Even if a metal is not directly in contact with a more oxidizable metal, oxidation of the least thermodynamically favorable metal is still likely to occur. To better reveal the oxidation behavior of solid solutions, free energy expressions derived from thermodynamics of solutions need to be considered.

W.A. Brantley: The authors suggest that regions on the alloy surfaces with substantial topography, such as sharp corners (and other sites with small radii of curvature), will undergo partial softening/melting during the porcelain firing cycles and that this process will aid the development of intimate metal-ceramic interaction. Such a process would require melting or softening at temperatures that are several hundred degrees below the normal melting point of the casting alloy. Can the authors provide supporting information for this hypothesis? Could sufficient surface diffusion without softening/melting occur at elevated temperatures to yield the same result?

Authors: Our suggestion of partial softening/melting of sharp topographical features on heat treated alloy sur-

faces is based mainly upon the appearance of microstructural features after the porcelain firing cycle. Undoubtedly, similar features, such as, rounding of sharp corners etc., can result by surface diffusion in a fashion analogous to solid state sintering of porcelain powder (which occurs much below the firing temperature of the porcelain), and might have a role here in developing the observed features. However, instances with porcelain firing cycles which start at low temperature at a rapid heating rate to a high temperature, which is significantly below the melting point of the alloy, may not be high enough for this phenomena to occur. Considerations regarding surface preparation again need to be given here. Since the alloy surfaces were alumina air abraded prior to porcelain firing, a high strain energy was introduced in the surface layer along with some compositional changes due to preferential abrasion of softer phases by impinging alumina particles and its retention on the surface. Such changes conceivably can cause localized melting at temperatures lower than the melting point of the alloy.

E. Papazoglou: For the Pd-Cu-Ga alloy Naturelle, you show a diffusion distance of 6 μm in the porcelain for the elements Cu, Ga, and Pd, suggesting chemical bonding. Do you have any evidence that for this alloy mechanical bonding is not important?

Authors: It was not our intent to reduce the role of mechanical bonding. If Pd-Cu nodules are not present in large numbers after porcelain firing to anchor the porcelain, interaction between alloy and porcelain still occurred by diffusion of Pd, Cu and Ga. This interaction by diffusion, however, does not automatically mean strong bonding between alloy and porcelain. Studies relating elemental diffusion to bond strength are in order.

E. Papazoglou: For the Pd-Ag alloy Jelstar, you do not mention if you observed interdiffusion of elements and to what depth. Mackert *et al* (1983) described a mechanical adherence mechanism for Will-Ceram W-1, an alloy with similar composition to Jelstar. They studied metallographically polished specimens that were oxidized and the formation of nodules was shown. Note that W-1 has 1 wt.% In in contrast to Jelstar which contains 6 wt.% In. Additionally, after mechanical testing they found that porcelain tags remained between the nodules. Employing X-ray diffraction and Auger electron spectroscopy, they proved that the nodular material did not contain oxides. Given the fact that your specimens were air abraded, and the existence of evidence (Brantley *et al.*, 1996) that air abrasion versus metallographic polishing might induce the formation of different oxide species for the high-palladium alloys, can you support your con-

jecture about the mechanical bonding with the evidence presented in your study?

Authors: The reason for not mentioning the depth of interdiffusion of elements in porcelain in this system was uncertainty due to the peak interferences from K in porcelain and Sn and In in alloy. Though, it was revealed that Pd and Ag diffusion occurred to about 1 μm in porcelain and Sn and In diffusion to about 2 μm . We agree that metallographic polishing and air abrasion produce surfaces with different compositions. Different oxides are likely to be produced depending upon the air abrasion techniques used. Evidence relating oxide-free surfaces to mechanical bonding and oxide-containing surfaces to chemical bonding is not established. Therefore, it is not unusual to speculate here that porcelain bonding occurred to Jelstar by mainly mechanical bonding, since the nodules appear to be favorable sites for mechanical anchoring and interlocking porcelain. Even if the nodular material became oxidized by the air abrasion, mechanical bonding may still have occurred.

E. Papazoglou: Given the inability to provide accurate elemental analyses for areas smaller than 1 μm with the EDS due to the existence of the interaction volume, can you conclude that submicron particles found in Acclaim near the surface after oxidation (Fig. 9) are Mn rich in the center and In rich in the periphery? For the same alloy, you found that In and Mn were diffused into the porcelain up to a distance of 4 μm . From these findings, can you make a conclusion about the mechanical nature of the bond for Acclaim?

Authors: It is true that the detailed elemental analyses cannot be accurately performed when the particles in question have small dimensions (1 μm). Yet, a qualitative statement can be made whether a particular area is rich, poor or devoid of a particular element when compared with the matrix. The darker shade particles were Mn-rich and lighter gray particles were In-rich, and some particles were Mn-rich in the center and In-rich at the periphery. Still, we feel that the latter part of the statement can be deduced from the observation that if separate dark gray and light gray areas are Mn-rich and In-rich, respectively, than the single area of darker center and lighter periphery should be Mn-rich and In-rich, respectively. There may be porcelain/alloy systems where the bonding can exclusively be of mechanical nature, but never exclusively of chemical nature as there will always be a mechanical component present at the interface. In the absence of a suitable technique for determining the bonding component, one can only reason based upon observation about the predominant component. Since the surface structure of heat treated Acclaim was largely similar to Jelstar, and to which porcelain adhered by forming interlocks, we suggested a predomi-

nant mechanical nature of bond between Acclaim/Porcelain even though Mn and In diffused to 4 μm . Although, diffusion of alloy elements into porcelain occurred, inference of strong chemical bonding does not automatically follow. Very likely, there is a chemical component (maybe significant) of bonding associated with the mechanical component.

E. Papazoglou: For the Au-Pd alloy SMG-3, you refer to 1 μm diffusion of Sn and Pd in the porcelain. Again, given the inability to provide accurate elemental analyses for areas smaller than 1 μm with the EDS, can you say that SMG-3 bonds basically due to chemical interaction?

Authors: The surface of heat treated SMG-3 was not similar to the surfaces seen in Jelstar and Acclaim. The oxidized surface of the former was largely smooth while the oxidized surfaces of the latter alloys were largely covered with nodules. Based on this observation, diffusion of alloying elements in the porcelain was taken as the main component of bonding, in this case chemical.

E. Papazoglou: Could you make predictions for the bond strength or porcelain adherence for the alloys in this investigation from the findings presented?

Authors: Bond strength is directly related to bonding forces developed by both mechanical interlocking and chemical interactions. While one or both bonding mechanisms may be detected or observed, such as, in this investigation with the use of SEM and EDS, assurances cannot be put forth regarding the strength of the bonds formed. The strength of mechanical interlocks can be affected by not only how well the fused porcelain has undermined the oxide or nodule interlocks, but also by the attachment of the oxide or nodule interlocks to the substrate alloy. With weak oxide or nodule attachment, a low bond strength may still occur even though the porcelain is firmly anchored to the outer oxides or nodules. Similarly, with chemical interactions, diffusion of alloy constituents may have occurred well within the porcelain, but presents no assurances that strong chemical bonding exists. Studies relating the modes of bonding, such as observed in this investigation, to bond strengths are in order.

Additional Reference

Mueller HJ (1996) Effect of surface preparation on high temperature oxidation of Ni-Cr-Be and Co-Cr alloys. *Microstruc Sci*, 23, 197-205.